Geology of Ore Deposits, Vol. 46, No. 1, 2004, pp. 64–75. Translated from Geologiya Rudnykh Mestorozhdenii, Vol. 46, No. 1, 2004, pp. 74–87.

Fluid Inclusions in Minerals from Modern Sulfide Edifices: Physicochemical Conditions of Formation and Evolution of Fluids

N. S. Bortnikov*[1], V. A. Simonov, and Yu. A. Bogdanov*****

**Institute of Geology of Ore Deposits, Petrography, Mineralogy, and Geochemistry, Russian Academy of Sciences, Staromonetnyĭ per. 35, Moscow, 119017 Russia*

***United Institute of Geology, Geophysics, and Mineralogy, Siberian Division, Russian Academy of Sciences, pr. Akademika Koptyuga 3, Novosibirsk, 630090 Russia*

****Shirshov Institute of Oceanology, Russian Academy of Sciences, Nakhimovskiĭ pr. 36, Moscow, 117218 Russia*

Received November 4, 2002

Abstract—A study of fluid inclusions in minerals (anhydrite, barite, and opal) from modern seafloor sulfide edifices located on the slow-spreading Mid-Atlantic Ridge (the Logachev-1, Rainbow, and Broken Spur hydrothermal fields) and in the Manus (Vienna Wood) and Woodlark basins in the southwestern Pacific was carried out. Fluid inclusions of 5–25 μm in size are two-phase at room temperature and contain liquid and a vapor bubble. Only anhydrite from the Logachev-1 hydrothermal field contains three-phase fluid inclusions (liquid, a vapor bubble, and solid) and vapor-rich fluid inclusions. It was found that dissolved NaCl prevails in fluids trapped in the inclusions, while KCl is a minor constituent. Variations in the salt concentration in trapped fluids were revealed and found to lie within the following ranges (in wt % NaCl-equiv.): 4.2–~26 in the fluids circulated in the Logachev-1 hydrothermal system; 4.1–8.5 in the Rainbow field, 3.0–6.3 in the Broken Spur field, 1.6–7.6 in the Vienna Wood field, and 2.7–6.9 in the system within the Woodlark basin. Homogenization temperatures of fluid inclusions varied from 102 to 398°C. It was shown that the range of mineral formation temperatures and fluid salinity estimated from thermometric measurements of fluid inclusions is much wider than that obtained by direct measurements for fluids venting onto the seafloor. Variations of fluid salinity were assumed to be caused by fluid separation at a temperature near or above the critical temperature of seawater, which leads to brine formation in modern hydrothermal systems.

INTRODUCTION

Our knowledge of the physicochemical parameters and chemistry of mineral-forming fluids responsible for the formation of sulfide edifices at oceanic spreading zones is mainly based on results of direct temperature measurements using submersibles, analysis of the fluids discharging onto the seafloor from vents of black smokers, and data of thermodynamic and experimental modeling. Monitoring of active hydrothermal fields located on mid-oceanic ridges showed that the temperature, pH, and salt content in fluids change with time (Von Damm *et al.*, 1997). A decrease in temperature (by 10–15°C), pressure, and chlorine and dissolved volatile contents over several years was revealed. A study of the sequence of deposition of mineral assemblages in seafloor sulfide edifices revealed successive mineral replacements and allowed us to assume a decrease in mineral formation temperatures from 370 to 240°C or lower during the growth of one edifice and even one chimney (Bortnikov and Lisitsyn, 1995). These changes are apparent because the direct measurements allow one to estimate the evolution of the physicochemical parameters and composition of fluids for short periods (several years), while sulfide edifices grow over several thousands to tens of thousands of years (Lalou *et al.*, 1993).

It is of interest to find out to what extent the fluid temperature and composition change in active seafloor systems during the period of their activity. These data can be obtained by study of fluid inclusions in minerals, because this technique permits quite reliable estimation of physicochemical parameters of hydrothermal systems (Roedder, 1984). It should be emphasized that the study of fluid inclusions in minerals from seafloor sulfide edifices provides new evidence for the high reliability of this technique.

Data on fluid inclusions in minerals from sulfide edifices are sparse (Naumov *et al.*, 1991; Simonov *et al.*, 1997, 2002; Le Bel and Oudin, 1982; Peter and Scott, 1988; Nehlig, 1991; Binns *et al.*, 1993), because the small sizes of fluid inclusions make it difficult to perform thermometric measurements. In order to compensate for the lack of available data, we studied fluid inclusions in minerals from sulfide edifices located on the slow-spreading Mid-Atlantic Ridge (the Logachev-1, Rainbow, and Broken Spur hydrothermal fields) in different geological settings and in the Manus and Wood-

[1]Corresponding author: N.S. Bortnikov. E-mail: bns@igem.ru

lark basins of the southwestern Pacific. The examined samples were collected during dives of Mir submersibles during cruises of the R/V *Akademik Mstislav Keldysh* (Lisitsyn *et al.*, $1992_{1,2}$; Bogdanov *et al.*, 1997, 1999). The data obtained are considered in this paper.

CHARACTERIZATION OF HYDROTHERMAL FIELDS AND MINERAL ASSEMBLAGES

A characterization of hydrothermal fields studied and mineral assemblages is given in Table 1. Data on the crystallization sequence of mineral aggregates and minerals in which the examination of fluid inclusions was possible are considered below.

Several hydrothermal fields associated with rocks of different composition were found on the Mid-Atlantic Ridge (Fig. 1a). Some of them (Lucky Strike, Broken Spur, TAG, and Snake Pit) are confined to neovolcanic zones and linked with domes composed of normal basalts of mid-oceanic ridges (N-MORB). Other hydrothermal fields (Rainbow, Logachev-1, and Logachev-2) are related to serpentinites uplifted to the seafloor along rifts and faults.

In the Logachev-1 hydrothermal field, some chimneys built up on a sulfide mound display concentric zoning (Bogdanov *et al.*, 1997). The concentric zoning around feeder channels is expressed in the growth of chalcopyrite dendrites and sphalerite crusts on the walls of ellipselike, spherical, and irregularly shaped holes filled with amorphous silica, sphalerite, and chalcopyrite. Open or completely sealed channels are rimmed by thin zones composed of chalcopyrite, isocubanite, and sphalerite. The next zone consists of sphalerite, chalcopyrite, marcasite, and pyrite with pyrrhotite relicts. The groundmass of the edifice consists of fine-grained (less than 50 μm) mineral aggregates, while grain sizes increase and reach several millimeters around the channel. Clusters of medium-grained anhydrite were found within sulfide aggregates. Anhydrite is replaced by sulfides, which indicates an earlier deposition of the sulfate mineral. Mutual intergrowth of anhydrite and sulfides was also observed, suggesting coeval crystallization of these minerals. Microdruses (up to 10 mm in size) of small anhydrite crystals line the walls of holes among the sulfide aggregates.

These observations indicate multiple deposition or redeposition of anhydrite during the formation of the edifice. In general, the sequence of mineral deposition during the chimney growth was as follows: anhydrite was the earliest to crystallize, followed by fine-grained pyrrhotite–sphalerite aggregates and then by chalcopyrite–isocubanite aggregates, while marcasite and sphalerite crusts completed the mineral deposition.

In the Rainbow hydrothermal field, the sulfide chimneys are zoned as well (Bogdanov *et al.*, 2002). The outer zones consist of fine-grained sphalerite aggregates. The central zones (around channels) are comprised of radially oriented chalcopyrite and isocubanite

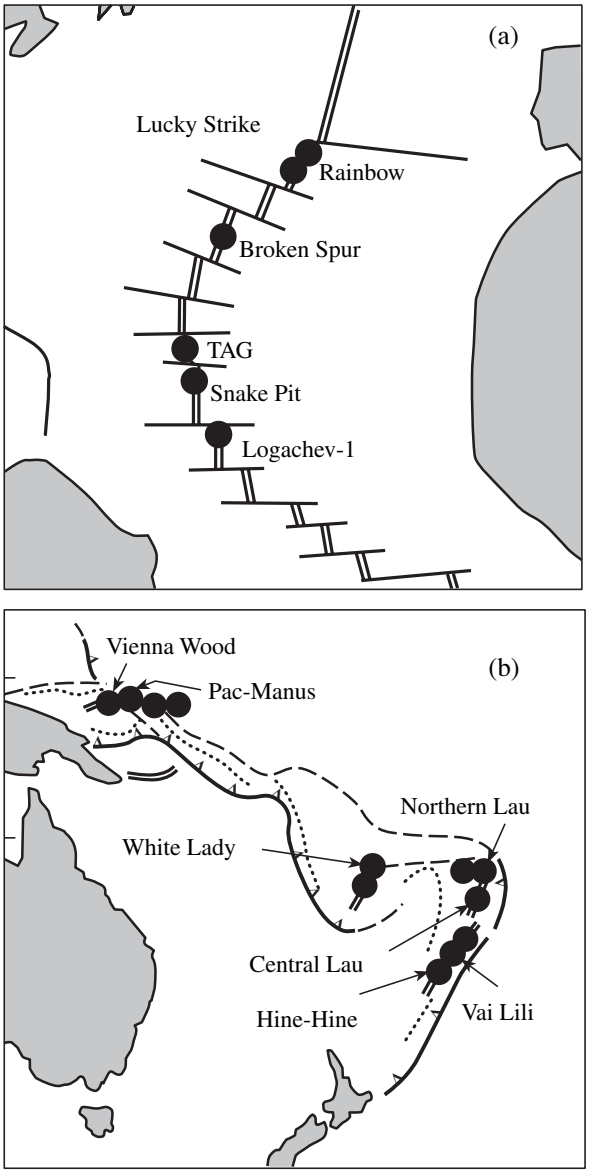

Fig. 1. Scheme of distribution of modern hydrothermal sites at the Mid-Atlantic Ridge (a) and in the back-arc basins of the Pacific Ocean (b).

grains with a lattice texture. The tops of active chimneys are composed of anhydrite–chalcopyrite aggregates. The edifice basements consist of massive fine- and ultrafine-grained sulfide aggregates. Several generations of anhydrite were found in the edifices. Anhydrite I forms the outer zones of the sulfide–anhydrite chimneys and, possibly, is the earliest mineral. Anhydrite II occurs as coarser grained aggregates observed as inclusions in areas between copper sulfide chimneys grown together. This anhydrite normally includes disseminated euhedral chalcopyrite crystals and small bornite grains. Anhydrite II fills radial cracks in the copper sulfide chimneys. This suggests that anhydrite II crystallized after the sulfide aggregates.

Table 1. Characterization of some modern seafloor hydrothermal fields in the world ocean

Name, location	Geological setting	Hydrothermal deposits	Mineralogy	References
		Mid-Atlantic Ridge		
Logachev-1, 14°45′ N	Thirty-five miles south of the transform fault at 15°20′ on the marginal slope of the rift valley. The western marginal slope of the rift valley is formed by a system of faults and composed of basalts; the eastern slope consists of gabbroids and serpentinized ultramafic rocks. Rock shearing and tectonic brecciation are widespread	The mound, 10–20 m high, ~200 m long, and up to 100 m wide, is mainly extinct; active vents are up to 10 m in diameter, and relict and active conical and spirelike chimneys 20–50 cm high are on the slopes and surface of the mound; the edifice is ~20 m in diameter, with age estimated as ~20–30 ka; active sulfide chimneys are built up on the basement, 2–5 m high, which is composed of low-temperature deposits, and inactive sulfide chimneys from 10 cm to 4 m high are found on the periphery; age is 50–65 ka	Pyrrhotite, sphalerite, chalcopyrite, isocubanite, pyrite, marcasite, bornite, Co pentlandite	Bogdanov *et al.*, 1997
Rainbow, 36°15′ N	Two hundred kilometers south of the Azores triple point; in the rift valley on the axis of the dome in the vicinity of its intersection with a transform displacement; the rift is framed by normal marginal tectonic benches; the axis dome is a serpentinite diapir	Relict single chimneys and groups and chains (10–15 m long) of sulfide chimneys 0.2–2 m high and up to 0.2 m in diameter at the base; active and relict edifices 12–20 m high and up to 5–10 m in diameter, the basement of which is surmounted by chimneys 10–12 cm to 3–4 m high; the length and width of the field are 250 and about 60 m, respectively	Pyrrhotite, isocubanite, chalcopyrite, sphalerite, pyrite, marcasite, bornite, millerite, nickeline	Bogdanov *et al.*, 2002; this study
Broken Spur, 29°10.2′ N and 43°10.3′ W	Neovolcanic ridge along the axis of a rift valley, composed of basalts and restricted by marginal tectonic benches, at a rift segment 61 km long located 100 km south of the Atlantis transform fault; age is <1000 years	Two types of sulfide edifices are found: (1) pilelike chimneys 0.5–1.0 to 18 m high and 0.3–1.0 m in diameter located on the volcanic basement; (2) sulfide tube- and melonlike edifices located on conical hills 15–37 m high and 10–20 m in diameter composed of fragments of sulfide ores	Pyrrhotite, pyrite, marcasite, sphalerite, würtzite, chalcopyrite, isocubanite, bornite, digenite, covellite, galena, jordanite, anhydrite, amorphous silica, barite, talc, lepidocrocite	Bogdanov *et al.*, 1997; Duckworth *et al.*, 1995; this study
		Southwestern Pacific		
Vienna Wood, Manus basin, 3°9.85′ S and 150°16.78′ E	Range of volcanoes in the axis zone of a linear segment of the rift valley; N-MORB tholeiitic basalts, rare back-arc basin basalts; tectonic extensional structures	Active and inactive sulfide and sulfate with sulfide tubelike and conical chimneys up to 14 m high	Sphalerite, würtzite, pyrite, marcasite, chalcopyrite, galena, Ag and Sb sulfosalts: pyrargyrite (?), stephanite (?), barite, amorphous silica	Lisitsyn *et al.*, $1992_{1,2}$; Schadlun *et al.*, 1992
Franklin seamount, Woodlark basin, 9°55′ S and 151°50′ E	Caldera and flank of axis volcano, confined to linear segment of spreading axis in basalt suite; spreading axis propagates into continental crust—rifting of continental crust	Barite–silica–sulfide chimneys a few meters high	Barite, silica, pyrite, sphalerite	Binns *et al.*, 1993; Lisitsyn *et al.*, $1992_{1,2}$

In the Broken Spur hydrothermal field, three types of ores were identified: (1) pyrrhotite-rich ores, (2) isocubanite–chalcopyrite-rich ores, and (3) chalcopyrite–pyrite (with marcasite) ores (Bogdanov *et al.*, 1997). The chalcopyrite–isocubanite-rich ores were found among fragments of thin-walled sulfide chimneys. In these chimneys, the inner walls are lined with fine-grained isocubanite crusts 1–5 mm thick, while the outer zones consist of tabular anhydrite crystals containing disseminated small dendrites of chalcocite,

marcasite, and chalcopyrite. In these zones, oval and angular fine-grained anhydrite aggregates are cemented by thinly rhythmical pyrite–marcasite aggregates. They contain rare disseminated small dendrites of pyrite and chalcopyrite. Such textural and structural relationships indicate the earlier deposition of anhydrite relative to the bulk of sulfide minerals. Small tubes about 4 cm in diameter with concentric zoning were also found in this hydrothermal field. Their inner zones consist of alternating thin sulfide and anhydrite–opal aggregates. The channel walls along which the hydrothermal fluids ascend consist of chalcopyrite and isocubanite partially replacing anhydrite (Bogdanov *et al.*, 1997; Duckworth *et al.*, 1995).

Of the hydrothermal fields discovered in the southwestern Pacific (Fig. 1b), we studied samples from the Vienna Wood sulfide edifice in the Manus basin and the barite–sulfide edifices on the Franklin seamount in the Woodlark basin.

The Vienna Wood sulfide edifice consists of a basement of sulfide crust up to 20 cm thick surmounted by several active and extinct tube- and spirelike chimneys (Bortnikov and Lisitsyn, 1995; Schadlun *et al.*, 1992). The chalcopyrite–pyrite–würtzite–sphalerite mineral assemblage with amorphous silica is the earliest in this edifice. The galena–sphalerite–pyrite–marcasite mineral assemblage including barite and silica was deposited later. On the basis of the essential dominance of barite over sulfide minerals in some small spirelike chimneys, we can distinguish a third, sulfide–barite assemblage. In addition to marcasite, sphalerite, and galena, this assemblage also includes anglesite, which probably crystallized as the latest mineral in small pores in an oxidized environment.

On the slopes of *the Franklin seamount in the Woodlark basin*, barite–silica–sulfide chimneys of a few meters in height were found (Binns *et al.*, 1993). The chimney walls are composed of barite and silica. Barite was the first mineral to crystallize. Sulfide minerals represented by pyrite spheroids and polycrystalline pyrite–sphalerite aggregates are occasional. They occur as inclusions in barite and silica.

SAMPLE DESCRIPTION

In the chimneys in the Logachev-1 hydrothermal field, fluid inclusions were studied in samples 3453-5b and 3454-1, representing fragments of tube walls 20 mm thick with rhythmical zoning. We observed more than 20 distinct bands (0.2–2 mm thick), composed of sulfide aggregates of variable composition. Sample 3454-1 was collected from a conical chimney with a zonal structure. The chalcopyrite zone is developed around the ellipselike open channel. The outer zone consists of bornite and digenite. Fluid inclusions were studied in early anhydrite, observed among sulfide aggregates as isolated clusters up to 1–2 mm in size or strips 0.1–2 mm thick and up to 10 mm long. Fluid inclusions were found in the late anhydrite of sample 3453-5a, which forms microdruses on walls of holes among sulfide aggregates and in aggregates of euhedral tabular transparent anhydrite crystals 0.3–1.5 mm in size. Open spaces are preserved among grains in these aggregates.

In an edifice within the Rainbow hydrothermal field, fluid inclusions suitable for microthermometric study were found in samples of three assemblages: (1) chalcopyrite–sphalerite–anhydrite aggregates (sample 3848-8-4a), (2) anhydrite–marcasite–chalcopyrite aggregates (sample 3840-8-6a), and (3) apoharzburgite serpentinite (sample 3844-3-4).

In sulfide chimneys from the Broken Spur hydrothermal field, fluid inclusions were found in three samples (3348-1, 3348-2a, and 3348-2b). The inclusions were examined in the anhydrite that composes thin crusts together with sulfide minerals. These crusts, 3–4 mm thick, form on walls of a tube about 15 mm in diameter (sample 3348-1). A sulfide (with anhydrite) crust 3–4 mm thick (sample 3348-2a) and elongated (8 × 20 mm) patches consisting of an aggregate of small (up to 1 mm) anhydrite crystals surrounded by a sulfide rim occur in sample 3348-2b.

In the Vienna Wood sulfide edifice, fluid inclusions were found in anhydrite from sulfide ore sampled at the top of a high active chimney (sample 2255-11), in druselike tabular barite crystals up to 1 mm in size (sample 2255-6), and in opaline silica from the sulfide aggregates (sample 2255-4) composing the basement of the edifice.

In the barite–sulfide edifice on the Franklin seamount, fluid inclusions were studied in barite containing disseminated sulfides (sample 2202-1A2).

ANALYTICAL TECHNIQUE

The phase composition of fluid inclusions was studied under a microscope. Their behavior on heating and freezing was examined using heating and freezing stages (Simonov, 1993). Fifty to a hundred values of homogenization temperatures were measured and about 30–50 values of salt contents were estimated for fluids trapped in inclusions in minerals from the ore types or mineral assemblages found in the sulfide edifices studied. The accuracy of determination of the temperatures for homogenization of fluid inclusions and melting of the last ice crystals and eutectics was controlled by replicate measurements. The error for homogenization temperature was ±2°C, while that for freezing temperature was ±0.2°C. The composition of the major salt components dissolved in the fluid was identified using the eutectic temperatures (Borisenko, 1977). The salt concentration in fluids trapped in fluid inclusions was calculated on the basis of the ice melting temperatures (Bodnar, 1993). It is known that the temperature of homogenization of fluid inclusions corresponds to the minimal temperature of mineral forma-

tion (Roedder, 1984). Thus, the estimation of the true temperature values of mineral formation requires a pressure correction that depends on pressure and fluid salinity. The true temperatures were calculated using a pressure correction value that was determined by adjustment of several correction values obtained by different methods (Lemmlein, 1973; Naumov, 1982; Roedder, 1984).

RESULTS

Description of Fluid Inclusions

Two-phase fluid inclusions 10–50 μm in size are uniformly distributed in crystals or oriented along one direction in the early anhydrite crystals from the edifice in the Logachev-1 hydrothermal field and are classified as primary. Fluid inclusions have the shapes of flat plates and regular rectilinear tubes.

The primary fluid inclusions of various shapes and sizes—tabular, up to 100 μm in size; ellipselike; and isometric, 40–60 μm in size—were previously identified in anhydrite from sample 3454-1. They were subdivided into several types by their phase composition at 25°C (Bortnikov *et al.*, 1997).

Three-phase fluid inclusions consisting of liquid, vapor, and several solids comprise type I. Solid phases are transparent and are identified as chloride salts by their optical properties.

Two-phase fluid inclusions composed of liquid and vapor are distinguished as type II.

Vapor-rich fluid inclusions are identified as type III. These inclusions normally have shapes of negative crystals or are spherical.

Fluid inclusions of the above three types are confined to the same growth zones of the mineral grains. This indicates that fluids of different compositions were trapped simultaneously.

Fluid inclusions of flat or spherical shape that contain only liquid are grouped in type IV.

Clusters of the primary, two-phase fluid inclusions (up to 50 μm in size) are uniformly distributed in crystals of late anhydrite from microdruses (sample 3453-5a). They are very thin, flat, and angular.

Primary fluid inclusions uniformly distributed within mineral grains or confined to the growth zones and pseudosecondary and secondary fluid inclusions confined to healed cracks were found in anhydrite microcrystals about 0.5–1 μm in size from the chalcopyrite–sphalerite–anhydrite aggregates from the edifice in the Rainbow hydrothermal field. The primary and pseudosecondary fluid inclusions, both regularly and variously shaped and 5–50 μm in size, were studied in detail. At 25°C, they normally consist of two phases, i.e., a light-colored liquid and a vapor bubble.

Primary fluid inclusions 5–40 μm in size distributed uniformly in crystals or oriented parallel to the elongation of the mineral grain are observed in anhydrite from anhydrite–marcasite–chalcopyrite aggregates. They normally look like rectilinear tubes or flat rectangles. They are also two-phase at 25°C and consist of light-colored liquid and a vapor bubble.

Very rare fluid inclusions (3–20 μm in size) are found in aragonite that composes veinlets in serpentinite. They are confined to healed cracks, thus indicating their secondary origin. These fluid inclusions display irregular and frequently elongated shapes. At 25°C, they mainly contain only one phase, with two-phase fluid inclusions of light-colored liquid and a vapor bubble are being less frequent.

Rare primary fluid inclusions 10–30 μm in size are found in anhydrite from the Broken Spur edifice (sample 3348-1). They are uniformly distributed, but are more abundant near the crystal core. Fluid inclusions are in the shape of flat or elongated plates. At 25°C, they contain two phases: a light-colored liquid and a vapor bubble. Rare primary fluid inclusions 10 μm in size, uniformly distributed over the crystal volume, are found in anhydrite from the sulfide–anhydrite crust (sample 3348-2a). Usually, they have the shape of elongated flat plates. Rare spherical two-phase primary fluid inclusions (up to 35 μm) were found in anhydrite that forms patches (sample 3348-2b).

Primary fluid inclusions 5–25 μm in size distributed uniformly within crystals were found in anhydrite (sample 2255-11) from the Vienna Wood sulfide edifice. Elongated platy fluid inclusions with poorly defined edges prevail among them. They are two-phase at 25°C and consist of light-colored liquid and a vapor bubble. Primary and secondary fluid inclusions were found in barite (sample 2255-6). Primary fluid inclusions are extremely rare. Several grains with a few inclusions (about 20 μm in size) were found among several hundred grains examined. These fluid inclusions are isometric with unclear edges. They are two-phase at 25°C and consist of a light-colored liquid and a dark spherical vapor bubble. Secondary fluid inclusions are predominant in the barite grains examined. These fluid inclusions, 3–10 μm in size, are confined to healed cracks and generally have flat shapes. One- and two-phase fluid inclusions in which the light-colored liquid and vapor bubble prevail were encountered among them at 25°C. These fluid inclusions are frequently located close to each other. Quite unusual fluid inclusions 10–30 μm in size were found in doubly polished thin sections of opaline silica (sample 2255-4) at high magnification. The shape of these fluid inclusions, with concave walls, is caused by the specific texture of the silica aggregate, consisting of closely-packed spherical micrograins. Actually, the fluid inclusions themselves fill residual intergranular spaces between microballs, where silica-forming fluids were encapsulated. They are two-phase at 25°C and contain a light-colored liquid and small vapor bubbles.

Primary fluid inclusions (5–15 μm and up to 65 μm in size) located along the growth zones were found in

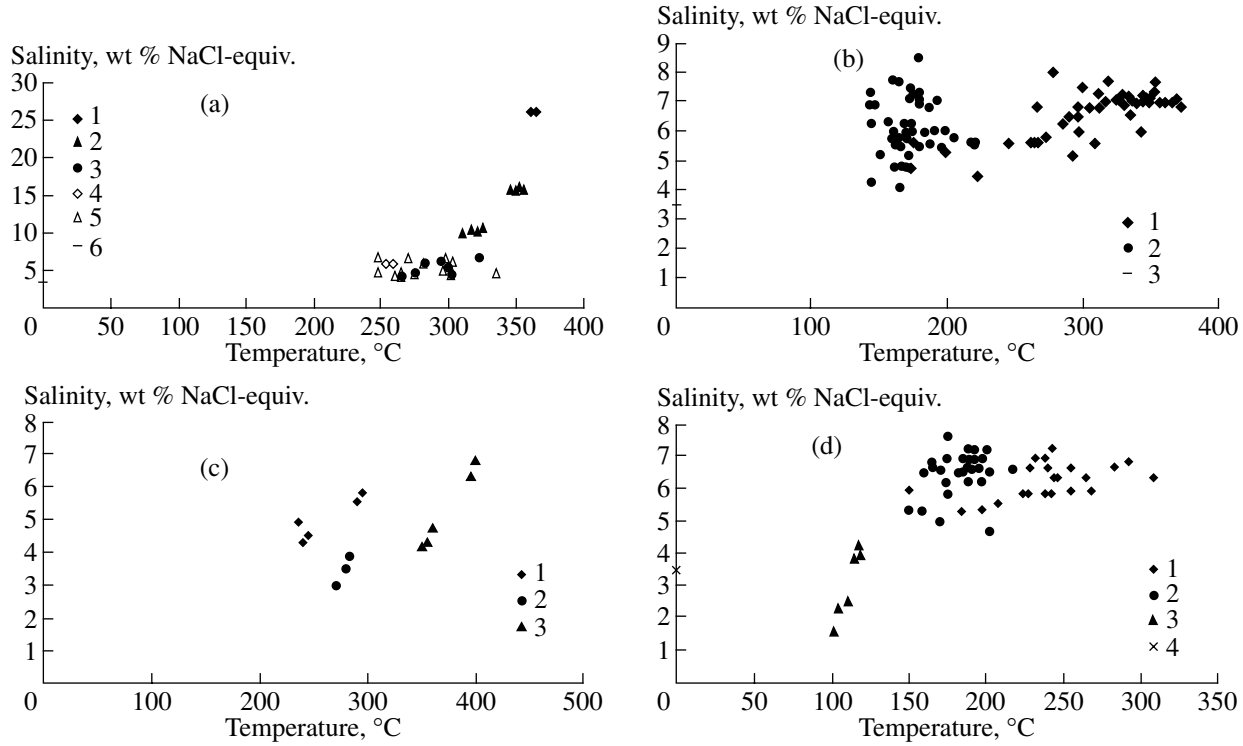

Fig. 2. Fluid salinity in fluid inclusions vs. homogenization temperatures. (a) Sulfide edifice in the Logachev-1 field: (1) type I fluid inclusions in anhydrite; (2–4) type II fluid inclusions in anhydrite I; (5) anhydrite II; (6) salinity of seawater under standard conditions (25°C). (1–3) After Bortnikov *et al.*, 1997; (4, 5) this study. (b) Sulfide edifices in the Rainbow field: (1) anhydrite from the anhydrite–marcasite–chalcopyrite assemblage; (2) anhydrite from the chalcopyrite–sphalerite–anhydrite assemblage; (3) salinity of seawater under standard conditions (25°C). (c) Sulfide edifices in the Broken Spur field: (1) sample 3348-1; (2) sample 3348-2a; (3) sample 3348-2b. (d) Vienna Wood sulfide edifice: (1) anhydrite; (2) barite; (3) opal; (4) salinity of seawater under standard conditions (25°C).

barite (sample 2202-1A2) from the barite–sulfide edifice on the Franklin seamount (Woodlark basin). They are two-phase at 25°C and contain a light-colored liquid and a spherical vapor bubble.

Microthermometric Studies

Logachev-1 field. The study of type 1 fluid inclusions showed (Bortnikov *et al.*, 1997) that salt crystals in the fluid inclusions with entrapped solid phases identified as halite by their optical properties disappeared by +25°C. We can assume that the salt content in the trapped fluid reached 26 wt % NaCl-equiv. Their homogenization occurred at 363°C (Fig. 2a).

The freezing of the type 2 fluid inclusions in the early anhydrite from the edifice in the Logachev-1 hydrothermal field showed that the eutectic temperatures ranged from –24.8 to –25.2°C. This indicates that NaCl prevails in the fluids trapped by these inclusions but a KCl admixture is also present. The ice melting temperatures vary from –2.4 to –12.3°C (Bortnikov *et al.*, 1997; this study). Thus, the salt content in the fluid is 4.2–16.2 wt % NaCl-equiv. On heating, these fluid inclusions were homogenized at 254–355°C. Taking into account the pressure correction corresponding to the sampling depth (3000 m), we can estimate the temperatures of hydrothermal mineral formation at 277–365°C.

As seen in Fig. 2a, fluids with higher salt contents are higher temperature, while those with low salinity are lower temperature. Such a relation between salinity and temperature indicates mixing of contrasting fluids: high-temperature brines with low-temperature dilute fluids (Roedder, 1984).

The eutectic temperatures of fluid inclusions in the late anhydrite were reached at –21.5 to –23.0°C. This indicates that dissolved NaCl prevails in the fluid trapped by them, while Na_2SO_4 is present as a minor constituent. The ice melting temperatures were –2.8 to –4.2°C. This indicates that the salt contents in the encapsulated fluid range from 4.3 to 6.7 wt % NaCl-equiv. The fluid inclusions were homogenized at 248 to 302°C and, rarely, at temperatures up to 336°C (Fig. 2a). Taking into account that the fluid was trapped by the growing crystals at a depth of about 3 km at a hydrostatic pressure of 300 bar, the pressure-corrected mineral formation temperatures were 271–322°C and up to 353°C.

Thus, the study of fluid inclusions showed that several immiscible phases and compositionally distinct

fluids circulated in the mineral-forming system of the Logachev-1 hydrothermal field at the physicochemical parameters at which deposition of anhydrite and associated minerals occurred. A high-temperature aqueous fluid containing up to 26 wt % NaCl-equiv. was among them. Its maximum temperature could reach 365°C. In addition to the liquid-rich fluid, a high-temperature vapor also circulated in the system. Its chemical composition has not been determined precisely, but we believe that aqueous vapor prevailed in this fluid. The temperatures of the vapor phase were identical to those for the liquid-rich fluid, which indicates their simultaneous trapping and formation by separation of one parental fluid into two phases upon a pressure drop. In general, the anhydrite deposition occurred from a fluid with salt contents of from 4.5 to 6.5 wt % NaCl-equiv. at 270–350°C.

Rainbow field. The fluid trapped in fluid inclusions in anhydrite from the chalcopyrite–sphalerite–anhydrite aggregates from the Rainbow edifice was frozen at –39 to –43°C. The eutectic temperatures, equal to –22.5 to –23.6°C, indicate that dissolved NaCl prevails in the trapped fluid, while minor amounts of Na_2SO_4 and, possibly, KCl also occur. The ice melting temperatures (–2.7 to –5.6°C) show that the salt content in the fluid was 4.1–8.5 wt % NaCl-equiv. Fluids with salinities of 4.1–7.7 wt % NaCl-equiv. are dominant. On heating, the homogenization of fluid inclusions occurred at 143–230°C, mainly, at 143–186°C (Fig. 2b). Because the ocean depth at the sampling site is about 2300 m, the true temperatures of anhydrite deposition in the chalcopyrite–sphalerite–anhydrite aggregates were about 160–200°C.

Fluid inclusions in anhydrite from the anhydrite–marcasite–chalcopyrite aggregates freeze at –37 to –44°C. The eutectic temperatures are –22.6 to –25.5°C. Thus, dissolved NaCl prevails in the trapped fluid, with minor amounts of KCl and, possibly, Na_2SO_4 also present. The ice melting temperatures, ranging from –2.9 to –5.0°C, indicate that the salt concentration is 4.5–7.7 wt % NaCl-equiv. Salinities from 5.3 to 7.7 wt % NaCl-equiv. are most frequent. On heating, fluid inclusions are homogenized at 245–372°C. In some cases, lower values of 170–174°C have been determined. Most fluid inclusions are homogenized at 282–365°C. The pressure-corrected temperature of anhydrite crystallization in this assemblage ranges from 295 to 370°C.

Fluid inclusions found in aragonite freeze at about –41°C, while the eutectic temperatures are –24.4 to –25.2°C. Thus, dissolved NaCl is predominant in the fluid trapped by these fluid inclusions and KCl is a minor constituent. The ice melting occurred at –1.8 to –2.4°C, which indicates a low salt content (2.7–3.7 wt % NaCl-equiv.) in the mineral-forming fluid. The homogenization temperatures of these fluid inclusions are 144–315°C. Given the ocean depth of about 2300 m, the true temperatures of aragonite crystallization can be estimated at 162–328°C.

Therefore, the salinity of fluids depositing the sulfide–sulfate ores in the Rainbow edifice was twice as high as the salinity of seawater. A wide variation in the crystallization temperature is typical of mineral formation in the Rainbow hydrothermal field (Fig. 2b).

Broken Spur field. On cooling, the eutectic temperatures of fluid inclusions in anhydrite from sample 3348-1 were reached at –21.4 to –22.0°C. This indicates the predominance of dissolved NaCl in the trapped fluid. The ice melting temperatures, equal to –2.0 to –2.5°C, indicate low salt content in this fluid (3.0–3.9 wt % NaCl-equiv.). The homogenization of fluid inclusions occurred at 271–283°C (Fig. 2d). Because the ore deposition occurred at a depth of about 3000 m, the crystallization temperature of hydrothermal minerals was 294–305°C. In anhydrite from the sulfide–anhydrite crust, the ice melting temperatures, from –3.2 to –3.7°C, indicate that the salt content in the trapped fluid was 4.9–5.8 wt % NaCl-equiv. The homogenization temperatures of these fluid inclusions varied from 236 to 295°C. The mineral formation temperatures are estimated at 259–317°C. Melting of ice crystals in fluid inclusions in the anhydrite composing patches occurred at –2.7 to –4.0°C. Thus, the salt concentration in the fluid was equal to 4.2–6.3 wt % NaCl-equiv. Homogenization of fluid inclusions occurred at 350–355°C and 394–398°C. The mineral formation temperatures are estimated at 368–373°C and 402–406°C.

Therefore, fluid with a salinity ranging from 3.0–6.3 wt % NaCl-equiv. (Fig. 2d) circulated in the mineral-forming system in the Broken Spur hydrothermal field, and the true temperatures of mineral formation were 259–406°C. The direct measurements showed that the maximum temperature of the fluids discharged onto the seafloor at the Broken Spur hydrothermal field was 366°C (Duckworth *et al.*, 1995). This is much lower than the temperatures obtained by fluid inclusion study.

Vienna Wood edifice. Fluid inclusions in anhydrite, barite, and opaline silica from the Vienna Wood edifice were examined.

On cooling of fluid inclusions in anhydrite (sample 2255-11), the fluid trapped in them freezes at –36 to –43°C, and the eutectic temperatures are reached at –22.2 to –25.7°C. This indicates that the inclusions contain aqueous fluid containing predominantly dissolved NaCl with a minor amount of KCl. The ice melting temperatures, equal to –3.4 to –4.6°C, indicate that the salt concentration in the fluid is 5.3–7.2 wt % NaCl-equiv. On heating, most fluid inclusions are homogenized at 224–268°C (Fig. 2c). Fluid inclusions with higher homogenization temperatures (up to 308°C) were also found in this sample. If the homogenization temperatures of fluid inclusions increase, the salt concentrations in the trapped fluid also increase. The temperatures corrected for a pressure of the water column

of about 250 bar at the mineral formation depth varied from 242 to 285°C, occasionally reaching 324°C.

On cooling, liquid in primary fluid inclusions in barite sample 2255-6 froze at about –41°C, while the eutectic temperatures were –23.5 to –24.6°C. Thus, the aqueous fluid in the fluid inclusions is dominated by dissolved NaCl and KCl is a minor constituent. The ice melting temperature (about –4.2°C) indicates that the salt concentration in the fluid is about 6.6 wt % NaCl-equiv. Fluid inclusions are homogenized at 216°C. Taking into account the pressure correction, the temperature of the barite deposition is estimated at 235°C.

Cooling of secondary fluid inclusions in barite showed that the fluid enclosed in them freezes within a wide temperature range, from –30 to –45°C. The eutectic temperatures are –23.2 to –25.7°C and indicate that dissolved NaCl prevails in the trapped fluid, while KCl is present as a minor constituent. The ice melting temperatures are from –3.0 to –4.9°C. Thus, the salt concentration in the fluid is 4.7–7.6 wt % NaCl-equiv. Fluid inclusions homogenized at 165–210°C predominate.

On cooling, fluids in fluid inclusions in opaline silica froze at about –41.5°C, while the eutectic point was reached at –24.1 to –25.7°C. Therefore, dissolved NaCl prevails in the fluid trapped by the inclusions, while KCl is a minor constituent. The relatively high temperature of ice melting (–1.1 to –2.7°C) indicates that the fluid encapsulated in the fluid inclusions was diluted: the salt content was 1.6–4.2 wt % NaCl-equiv. On heating, homogenization of fluid inclusions occurred at 102–118°C. Taking into account the pressure correction (the basin depth of about 2500 m), the temperatures of the silica formation are estimated at 128–145°C.

The edifice on the Franklin seamount. The eutectic temperatures of –22.3 to –23°C measured for primary fluid inclusions in barite from the sulfide–sulfate edifice on the Franklin seamount (sample 2202-1A2) indicate that dissolved NaCl prevails in the aqueous fluid trapped by inclusions, while KCl is a minor constituent. The salt concentration estimated by ice melting temperatures was 2.7–6.9 wt % NaCl-equiv. Homogenization of fluid inclusions occurred at 185–302°C. Differences in the fluid composition and homogenization temperatures of fluid inclusions in the inner and outer growth zones of barite were found. In the inner zone inclusions, the salt content is lower (2.7–3.3 wt % NaCl-equiv.) and homogenization temperatures are 200–205°C; in the outer zone inclusions, the fluids have higher salinity (5.4–6.9 wt % NaCl-equiv.), and their homogenization occurred at 185–302°C. The pressure-corrected temperatures for barite crystallization range from 203 to 316°C. In general, the values obtained are consistent with previously published data, i.e., homogenization temperatures of 184–244°C and a salinity of the trapped fluid of 3.4–5.8 wt % NaCl-equiv. (Binns *et al.*, 1993). It turns out that the temperature interval of mineral crystallization estimated by thermometric study of fluid inclusions differs from that determined by direct measurements for the mineral-forming fluid (270–350°C) and the salt concentration in the entrapped fluid varies within a much wider interval than that in the discharged fluid (4.0–4.7 wt %) (Gordeev, 1992).

Therefore, the study of fluid inclusions showed that the sulfide–sulfate edifice on the Franklin seamount was formed at 203–316°C from an aqueous fluid with dissolved NaCl and KCl and that the salt concentration varied from 2.7–6.9 wt % NaCl-equiv. The salinity of fluids increased by two times, and their maximum salt concentrations are twice as high as that in seawater.

DISCUSSION

The data obtained show that the study of fluid inclusions in minerals from modern sulfide edifices helps us to elucidate the composition and evolution of the mineral-forming fluids and the physicochemical conditions of mineral formation in hydrothermal systems operating in modern oceanic spreading zones. These investigations allow us to compare the physicochemical parameters of modern mineral-forming processes estimated by microthermometric studies with the data of direct measurements of the temperature and composition of hydrothermal fluids discharging from black smoker vents in active hydrothermal fields. This comparison is very important for drawing conclusions regarding ancient ore-forming processes from data of fluid inclusion studies.

In some cases, the temperatures of mineral formation estimated from fluid inclusions are consistent with data of direct measurements (Table 2). For instance, the highest temperatures of the hydrothermal fluid (295–370°C) depositing sulfide ores in the Rainbow hydrothermal field as estimated from fluid inclusions are close to the values of direct temperature measurements (250–362°C) (Bogdanov *et al.*, 1999). The mineral formation temperatures of anhydrite from the Vienna Wood edifice (Manus basin) estimated from fluid inclusions (242–285°C) are also compatible with the results of direct measurements of the discharging fluids (275°C) (Lisitsyn *et al.*, $1992_{1,2}$). However, the study of fluid inclusions shows that products of mineral formation at lower temperatures also occur in edifices of these hydrothermal fields, i.e., 130–170°C for the Rainbow field and 160–200°C for the Vienna Wood edifice.

The temperatures estimated by fluid inclusion studies differ from the directly measured values for some hydrothermal fields. For example, the temperatures of mineral formation in the Broken Spur field estimated from fluid inclusions vary from 259 to 406°C. The highest directly measured temperature of the fluids venting onto the seafloor was lower than the maximum value of the above interval and did not exceed 366°C. The study of fluid inclusions indicates that mineral formation in this field also occurred at lower temperatures (260–300°C). The temperatures of mineral formation in

Table 2. Comparison of fluid temperature and salinity in modern hydrothermal systems based on data of fluid inclusion study and direct measurements

Hydrothermal field, area	Results of fluid inclusion study		Data of direct measurements		References
	T_{cryst}, °C (T_{hom}, °C)	C, wt % NaCl-equiv.	T, °C	C_{Cl}, mmol/kg	
Logachev, MAR	270–365 (248–355)	4.2–26	>353	515–522	This study; Bogdanov *et al.*, 2002; Bortnikov *et al.*, 1997
Rainbow, MAR	160–370 (143–365)	4.1–8.5	250–362	753	This study, Bogdanov *et al.*, 2002
Broken Spur, MAR	259–406 (236–398)	3.0–6.3	366	469	Same
Vienna Wood, Manus basin	128–324 (102–308)	1.6–7.6	275		This study
Franklin seamount, Woodlark basin	203–316 (185–302)	2.7–6.9	270–350		This study
	(184–244)	3.4–5.8			Binns *et al.*, 1993

Note: The chlorine content in seawater is 541 mmol/kg.

the sulfide–sulfate edifices on the Franklin seamount estimated by fluid inclusion study (203–316°C) are lower than the temperatures measured for discharging fluids (270–350°C) (Gordeev, 1992).

The thermometric study of fluid inclusions showed that the temperatures of mineral formation in active sulfide systems vary significantly more widely than was previously suggested. For example, the growth temperatures for different zones within a mineral can differ by 100°C (see data for barite from the edifice on the Franklin seamount). The direct measurements have revealed variation in the temperature of the fluid discharging from black smokers. The fluid temperature at a black smoker vent on the East Pacific Rise at 9°16.8′ N was 388°C in 1991 and lower by 37°C (351°C) in 1994 (Von Damm *et al.*, 1997). A significant change in the temperature of mineral-forming fluids, from 202 to 333°C, was established in the Lucky Strike field (37°17′ N) (Mid-Atlantic Ridge) at depths of 1618–1726 m by measurements performed from 1993 to 1996. Even larger temperature variations were found by measurements with a 1-min interval using an autonomous thermometer at a vent in the Rainbow hydrothermal field. It was found that temperature repeatedly oscillated between 250 and 348°C over 35 min (Bogdanov *et al.*, 2002).

The study of fluid inclusions has revealed that the salinities of the hydrothermal fluids depositing the sulfide–sulfate ores of the Rainbow edifice (up to 8.5 wt % NaCl-equiv.) and the Vienna Wood edifice (up to 7.7 wt % NaCl-equiv.) were two times higher than the salt content in seawater. An even higher salinity of the mineral-forming fluid was recorded in the Logachev-1 hydrothermal system, where highly concentrated hydrothermal fluids with a salt content five times higher than that in seawater were found. The data obtained indicate that the fluids discharging from sulfide edifices on the ocean floor differ in composition from seawater, which is assumed to be the major component of the mineral-forming fluid in generally accepted models of seafloor hydrothermal systems.

The fluid salinity can increase during the transformation of seawater into mineral-forming fluid during its interaction with rocks of the oceanic lithosphere or fluid evolution during its ascent to the seafloor surface. It has been suggested that the salt concentration increases as a result of water consumption in the hydration reactions occurring during the amphibolite-facies metamorphism of the oceanic lithosphere (Cathles, 1983; Kelley and Delaney, 1987). The serpentinization of ultramafic rocks that is very abundant in some hydrothermal fields (Logachev-1 and Rainbow) could increase the salt concentration in the fluid produced in this process. Serpentinization is olivine hydration resulting in the formation of minerals of the serpentine group (antigorite, lizardite, and chrizotile) with accessory magnetite and brucite at 500°C. The process of membrane separation with water consumption occurs during these reactions, and the residual fluid is enriched in chlorides (MacDonald and Fife, 1985). Mixing of modified heated water with highly concentrated magmatic fluids could also increase the salinity of the mineral-forming fluid. The involvement of magmatic fluid was demonstrated for some seafloor hydrothermal systems in the Pacific back-arc basins (Binns and Scott, 1993; Herzig *et al.*, 1998, Kamenetsky *et al.*, 2001) and in the Mid-Atlantic Ridge (Simonov and Milosnov, 1996).

This phenomenon could be also accounted for by phase separation of supercritical or subcritical fluids in the deep zones of seafloor hydrothermal systems (Bishoff and Pitzer, 1985, Fournier, 1987; Delaney *et al.*, 1987; Goldfarb and Delaney, 1988; Bortnikov *et al.*, 1997). The model of fluid phase separation in seafloor hydrothermal systems was first employed to explain the

composition of volatile components in fluid collected on the East Pacific Rise at 21° N (Welham and Craig, 1979). The phase separation was confirmed by the study of syngenetic vapor-rich and highly concentrated liquid-rich fluid inclusions (Kelley and Delaney, 1987; Vanko, 1988; Bortnikov *et al.*, 1997). Seawater can be approximated by a H_2O–NaCl system. In this system, the composition of the fluid undergoing two-phase phase separation is restricted to a surface in the *PTX* diagram and the compositions of coexisting vapor and liquid are fixed at any given *P* and *T* (Bishoff and Pitzer, 1985; Fournier, 1987; Goldfarb and Delaney, 1988). The projection of the three-dimensional surface into the *PT* space represents a two-phase field, within which the compositions of coexisting vapor and liquid, being independent of the bulk salt concentration in the system, vary as functions of *P* and *T*. A curve separates the field of one-phase liquid from the two-phase field. The critical point at which vapor and liquid have identical properties and transform into a homogeneous fluid is not the endpoint of the two-phase curve in the H_2O–NaCl system. The critical point shifts to higher temperature and pressure with increasing bulk salt concentration in the fluid. Therefore, the style of fluid phase separation changes at the critical point: i.e., at *PT* conditions below the critical point, the vapor separates from the fluid intersecting the two-phase curve. Under *PT* conditions above the critical point, brines form due to condensation of the low-salinity vapor. The intrusion of magma into the oceanic lithosphere leads to its heating and convective circulation of water. In the off-axis hydrothermal systems at the Mid-Atlantic Ridge, such as those in the Logachev-1 field (Bogdanov *et al.*, 1997), seawater may penetrate to depths of 6–7 km and may be heated to temperatures higher than 450°C. Brines with a salinity of 19 wt % NaCl-equiv. and the vapor phase can originate if the fluid temperature exceeds 480°C (Fournier, 1987). It follows from Fig. 55.8 in the paper by Fournier (1987) that the fluid with the salt concentration of 26 wt % NaCl-equiv. trapped in fluid inclusions in anhydrite from the Logachev-1 edifice can originate as a result of phase separation if the ascending fluid crosses the condensation curve for seawater in the H_2O–NaCl system at a temperature higher than 510°C. However, it is generally assumed that the most favorable conditions for brine formation arise if the magma chamber is located at a depth of 3–4 km and the fluid temperature is below 450°C. Thus, the chlorine content in the fluid circulating in the hydrothermal system in the Rainbow field is similar to that in brine originating as a result of phase separation of a fluid with the salinity of seawater near the critical point for seawater at 407°C and 298 bar (Charlou *et al.*, 2002). Concentrations of salts both higher and lower than that for seawater were measured for fluids discharging from the Brandon sulfide edifice (East Pacific Rise, 21° S). The salinity variations are explained by phase separation at 405°C and 287 bar, i.e., under conditions below the critical point for seawater (Von Damm *et al.*, 2003).

Fournier (1987) showed that pore water could be heated up to 500–650°C if a magma was repeatedly intruded to a shallow depth. For example, heating of seawater to 500°C at a depth of 0.5 km from the seafloor below a 4-km water column results in formation of brines with 20 wt % NaCl-equiv. and a relatively dilute vapor. Highly concentrated brines are formed if seawater is heated up to 650°C at a depth of 9 km. The fluid (dilute vapor) will rise to the level of the seafloor, condense upon cooling, and mix with pore water. The brines will also rise, but their density will increase and their buoyancy decrease upon cooling. Due to its greater density, this fluid will accumulate in the deep zones of the hydrothermal systems. The brines may interact with convecting dilute fluid by diffusion (a steady layered double-diffusive model). As a result, the brine salinity decreases, while the hydrothermal fluid salinity increases (Bischoff and Rosenbauer, 1984, 1989). If the brine remains static, the highly concentrated fluid may be trapped by the slowly convecting overprinting fluid (Schoofs and Hansen, 2000). The gradual impoverishment of the brine layer leads to the origin of a hydrothermal fluid of a nearly constant salinity (approximately two times higher than the salinity of seawater). The stable discharge of high-salinity fluid from black smokers in the Rainbow hydrothermal field over a long period may indicate that a brine layer in which the salt content slowly and gradually decreases exists in a deep zone.

Variations in the salinity of mineral-forming fluid may be caused by change in rock permeability due to tectonic activity (Alt, 1995). The condensation results in a significant decrease in the salinity of the vapor-rich fluid also even if only small amounts of brines form. The NaCl partial molar volume in the solution is very large; thus, the bulk volume of the two-phase fluid increases significantly relative to the volume of the one-phase fluid. The increase in volume should be accompanied by fracturing (Goldfarb and Delaney, 1988). Brines will rise along these fractures to the seafloor surface, where they will mix with seawater. Their mixing with cold seawater results in variations in the fluid salinity during mineral deposition.

The circulation of two compositionally distinct fluids was revealed in the Logachev-1 and Vienna Wood hydrothermal systems. Their compositions are most contrasting in the Logachev-1 hydrothermal system. It is possible that boiling, or the separation of water vapor from the highly concentrated fluid, were recorded in this system.

Evidence for this phenomenon is the coexistence of liquid-rich and vapor-rich fluid inclusions. It is possible if highly concentrated (20–25 wt % NaCl-equiv.) high-temperature (about 400°C) fluid reached the seafloor surface at a water depth of about 3 km. Although no direct evidence for fluid phase separation was found in

samples from other hydrothermal sites, the variations in salinity of fluids circulated in these systems indicate that separation occurs. The compositions of fluids in the Vienna Wood system are not as contrasting as those in the Logachev-1 system. However, the correlation between fluid salinity and temperature testifies in favor of mixing of a hot, highly concentrated fluid with a relatively cold dilute fluid in this system during the mineral deposition.

The decrease in temperature by 37°C and fluid salinity by 1.5 times relative to seawater, which was recorded upon repeated measurement after three years, is interpreted as evidence of fluid separation (Von Damm *et al.*, 1997). It was suggested that the vapor phase originating due to separation rose to the seafloor just after volcanic eruption, while the liquid phase (brine) was filtered through the oceanic lithosphere for three years longer.

Therefore, the studies performed of fluid inclusions in minerals from sulfide edifices at modern seafloor hydrothermal sites allowed us to add significantly to knowledge of the thermal conditions of mineral crystallization, the composition of the mineral-forming fluids (mainly, the dissolved salt concentrations in them), and the nature of the evolution of mineral-forming fluid. New data obtained indicate that fluid separation can change the chemistry, in particular, the salinity of the initial mineral-forming fluid originating as a result of interaction of seawater with magmatic rocks of the oceanic lithosphere. Mixing of two fluids derived from distinct sources in a mineral-forming system also affected the fluid temperature and chemical composition.

ACKNOWLEDGMENTS

The authors thank V.Yu. Prokof'ev for critical comments during the preparation of the manuscript.

This study was supported by the Presidium of the Russian Academy of Sciences (the basic research program "The World's Ocean: Geology, Geodynamics, Physics, and Biology"); by the Ministry for Industry, Science, and Technology (the federal targeted program "The World's Ocean," state contract no. MO-11(OO)-P); and by the Russian Foundation for Basic Research (project nos. 00-05-65069 and 03-05-65045).

REFERENCES

1. J.C. Alt, in *Seafloor Hydrothermal Systems: Physical, Chemical, Biological and Geological Interactions*, Ed. by S. Humphrish (AGU, 1995) **91**, pp. 85–114.
2. R. A Binns and S.D. Scott, Econ. Geol. **88**, 2226 (1993).
3. R. A. Binns, S. D. Scott, Yu. A. Bogdanov, *et al.*, Econ. Geol. **88**, 2122 (1993).
4. J. L. Bishoff and K.S. Pitzer, Earth Planet. Sci. Lett. **75**, 327 (1985).
5. J. L. Bishoff and R.J. Rosenbauer, Earth Planet. Sci. Lett. **68**, 172 (1984).
6. J. L. Bishoff and R.J. Rosenbauer, J. Geol. **97**, 613 (1989).
7. R. J. Bodnar, Geochim. Cosmochim. Acta. **57**, 688 (1993).
8. Yu. A. Bogdanov, *Hydrothermal Sites at Rifts of Mid-Atlantic Ridge*, Nauchnyi Mir, Moscow, 1997) [in Russian].
9. Yu. A. Bogdanov, N.S. Bortnikov, and A. P. Lisitsyn, Geol. Rudn. Mestorozhd. **39**, 409 (1997) [Geol. Ore Deposits. **39**, 409 (1997)].
10. Yu. A. Bogdanov, N. S. Bortnikov, I. V. Vikent'ev, *et al.*, Geol. Rudn. Mestorozhd. **44**, 513 (2002) [Geol. Ore Deposits. **44**, 510 (2002)].
11. Yu. A. Bogdanov, A. M. Sagalevich, E. G. Gurvich, *et al.*, Dokl. Ross. Akad. Nauk **365**, 657 (1999) [Dokl. Russ. Acad. Sci. **365**, 657 (1999).
12. A. S. Borisenko, Geol. and Geophys. (8), 16 (1977) [in Russian].
13. N. S. Bortnikov and A. P. Lisitsyn, in *Geology and Mineral Resources in World Ocean*, Ed. by I. S. Gramberg (VNIIOceangeologiya, St. Petersburg, 1995), pp. 158–173 [in Russian].
14. N. S. Bortnikov, T. L. Krylova, Yu. A. Bogdanov, *et al.*, in *Mineral Deposits: Research and Exploration, Where do they meet?*, Ed. by H. Pappunen (Balkema, Rotterdam, 1997), pp. 353–356.
15. L. M. Cathles, in *The Kuroko and Related Volcanogenic Massive Sulfide Deposits. Econ. Geol. Mono 5*, Ed. by H. Ohmoto and B. J. Skinner (Soc. Econ. Geol., Inc., Chelsea, 1983), pp. 439–487.
16. J. L. Charlou, J. P. Donval, Y. Fouquet, *et al.*, Chem. Geol. **191**, 345 (2002).
17. R.C. Duckworth, R. Knott, A. F. Fallick, *et al.*, in *Hydrothermal Vents and Processes*, Ed. by I. M. Parson, C. I. Walker, and D. R. Dixon (Geol. Soc. Spec. Publ., London, 1995) **87**, pp. 175–189.
18. R. O. Fournier, US Geol. Surv. Spec. Paper **1350**, 1487 (1987).
19. M. S. Goldfarb and J. R. Delaney, J. Geophys. Res. **93** (1988).
20. V. V. Gordeev, in *Metallogeny of Modern and Ancient Oceans*, Ed. by A. P. Lisitsyn ("GEOEKSPORT," Moscow, 1992), pp. 181–183 [in Russian].
21. P.M. Herzig, M.D. Hannington, and A. Arribas, Jr., Mineral Deposita. **33**, 226 (1998).
22. D. S. Kelley and J. R. Delaney, Earth Planet. Sci. Lett. **83**, 53 (1987).
23. V. S. Kamenetsky, R. A. Binns, J. B. Gemmell, *et al.*, Earth Planet. Sci. Lett. **184**, 685 (2001).
24. C. Lalou, J. L. Reyss, E. Brichet, *et al.*, J. Geophys. Res. **98**, 9705 (1993).
25. L. Le Bel and E. Oudin, Chem. Geol. **37**, 129 (1982).
26. G. G. Lemmlein, *Morphology and Origin of Crystals* (Nauka, Moscow, 1973) [in Russian].
27. A. P. Lisitsyn, C. Krook, Yu. A. Bogdanov, *et al.*, Izv. Akad. Nauk SSSR, Ser. Geol. (10) 34 (1992) [in Russian].
28. A. P. Lisitsyn, O. P. Malakhov, Yu. A. Bogdanov, *et al.*, Izv. Akad. Nauk SSSR, Ser. Geol. (4) 5 (1992) [in Russian].
29. A. H. MacDonald and W. S. Fife, Tectonophysics. **116**, 123 (1985).

30. V. B. Naumov, in *Using of Thrmobarogeochemical Technique at Exploration and Study of Ore Deposits* (Nedra, Moscow, 1982), pp. 85–94 [in Russian].
31. V. B. Naumov, O. F. Mironova, V. Yu. Prokof'ev, and A. Yu. Lein, Geochemiya, No. 1, 39 (1991).
32. P. Nehlig, Earth Planet. Sci. Lett. **102**, 310 (1991).
33. J. M. Peter and S. D. Scott, Can. Mineral. **26**, 567 (1988).
34. E. Roedder, *Fluid inclusions* (Rev. in Mineralogy, Min. Soc. Amer., 1984), Vol. 12.
35. V. A. Simonov, *Petrogenesis of Ophyolites* (Thermochemical Study) (OIGGM, Novosibirsk, 1993).
36. V. A. Simonov, N.S. Bortnikov, and A. P. Lisitsyn, *Origin and Mining of Deposits in Ophyolites* (IMin UrO RAN, Miass, 2002), pp. 61–68.
37. V. A. Simonov and A. A. Milosnov, Geochimiya **8**, 760 (1996) [Geochim. Inernational. **8**, 760 (1996)].
38. T. N. Schadlun, N. S. Bortnikov, Yu. A. Bogdanov, *et al.*, Geol. Rudn. Mestorozhd. **34** (5), 3 (1992).
39. S. Schoofs and U. Hansen, Earth Planet. Sci. Lett. **180**, 341(2000).
40. D. A. Vanko, J. Geophys. Res. **93**, 4595 (1988).
41. K. L. Von Damm, L. G. Buttermore, and S.E. Oosting, Earth Planet. Sci. Lett. **149**, 101 (1997).
42. K. L. Von Damm, M. D. Lilley, W.C. Shanks III, *et al.*, Earth Planet. Sci. Lett. **206**, 365 (2003).
43. J. A. Welham and A. Graig, Geophys. Res. Lett. **6**, 829 (1979).